



Modeling and measuring the spatial relation “along”: Regions, contours and fuzzy sets

Celina Maki Takemura^{a,b}, Roberto M. Cesar Jr.^{b,*}, Isabelle Bloch^c

^a Embrapa Satellite Monitoring - Brazilian Agricultural Research Corporation, Av. Soldado Passarinho, 303, 13070-115 Campinas, Brazil

^b Institute of Mathematics and Statistics - IME, University of São Paulo - USP, Rua do Matão, 1010, 05508-090 São Paulo, Brazil

^c Télécom ParisTech - CNRS LTCI, 46 rue Barrault, 75013 Paris, France

ARTICLE INFO

Article history:

Received 21 December 2010

Accepted 3 June 2011

Available online 26 July 2011

Keywords:

Spatial relations

Spatial reasoning

Structural pattern recognition

ABSTRACT

The analysis of spatial relations among objects in an image is an important vision problem that involves both shape analysis and structural pattern recognition. In this paper, we propose a new approach to characterize the spatial relation *along*, an important feature of spatial configurations in space that has been overlooked in the literature up to now. We propose a mathematical definition of the degree to which an object *A* is along an object *B*, based on the region *between A and B* and a degree of elongatedness of this region. In order to better fit the perceptual meaning of the relation, distance information is included as well. In order to cover a more wide range of potential applications, both the crisp and fuzzy cases are considered. In the crisp case, the objects are represented in terms of 2D regions or 1D contours, and the definition of the alongness between them is derived from a visibility notion and from the region between the objects. However, the computational complexity of this approach leads us to the proposition of a new model to calculate the *between* region using the convex hull of the contours. On the fuzzy side, the region-based approach is extended. Experimental results obtained using synthetic shapes and brain structures in medical imaging corroborate the proposed model and the derived measures of alongness, thus showing that they agree with the common sense.

© 2011 Elsevier Ltd. All rights reserved.

1. Introduction

The importance of spatial relations between spatial entities or between parts of objects has been highlighted in many different works, including linguistics, philosophy, experimental psychology and computer science (see e.g. [2,8] for several references in different domains). For instance, according to feature integration theory, object perception requires the sequential allocation of focused attention to areas in space, enabling features belonging to the same object to be linked through their shared spatial location [20]. Moreover, relations between parts are main features for object perception and recognition [1,12,19]. The literature about the analysis of spatial relations from images is quite vast and dates back to the 1970s and 1980s [11,16]. In [11], Freeman presents mathematical–computational formalisms to represent the semantic context of terms (in English) that codify relationships between objects. Here we consider spatial relations between two spatial entities, that can be either different objects or different parts of one single object.

In the present paper we address the issue of modeling the relation *along*, which is a complex relation, not included in the usual basic topological or metric relations [13] and that has been overlooked by the computer vision literature. However, it is an important spatial relation that is often used to describe objects in natural language. Calculating the degree of alongness could be useful for processing spatial queries with natural language expressions [18] such as: “Which are the roads along the coast?” or “Which are the muscles along the femur?”. Structures along each other also appear in the context of thin objects in images. For instance, the edges of thin objects such as blood vessels or roads are inherently along each other. The use of this spatial relation may be useful to devise segmentation algorithms for thin structures. To the best of our knowledge, the only work addressing *alongness* between objects by giving mathematical definitions was developed in the context of geographic information systems (GIS) [18]. In that work, the relation *along* between a line and an object is defined as the length of the intersection of the line and the boundary of the object, normalized either by the length of this boundary (*perimeter alongness*) or by the length of the line (*line alongness*). In these definitions, the boundary can also be extended to a *buffer zone* around the boundary. However, no algorithmic implementations or real experimental results obtained from digital images are presented. Crevier [10] addresses the problem

* Corresponding author.

E-mail addresses: celina@cnpem.embrapa.br (C.M. Takemura), cesar@vision.ime.usp.br (R.M. Cesar Jr.), isabelle.bloch@telecom-paristech.fr (I. Bloch).

of spatial relationships between line segments by detecting collinear chains of segments based on the probability that successive segments belong to the same underlying structure. Nevertheless, this approach cannot be directly extended to any object shape. Here we consider the more general case where both objects can have any shape, and where they are not necessarily adjacent. For computer vision applications, the considered objects can be obtained for instance from a crisp or fuzzy segmentation of digital images. Algorithmic details for all approaches are provided.

The *along* relation is an intrinsically vague notion. Indeed, in numerous situations even of moderate complexity, it is difficult to provide a definite binary answer to the question “Is A along B ?”, and the answer should rather be a matter of degree. Therefore fuzzy modeling is appropriate, as for many relations that have an intuitively clear meaning but that defy any all-or-nothing mathematical definitions (see e.g. [3] for a review on fuzzy spatial relations). Now if the objects are themselves imprecisely defined, as fuzzy sets, this induces a second level of fuzziness.

In this paper, we propose a fuzzy model of the relation *along*, for both crisp and fuzzy 2D objects. It is based on a measure of elongatedness of the region *between* both objects. In case of crisp objects, they are considered as 2D shapes in images which, in turn, may be represented in terms of 2D regions or 1D contours. The 2D representation is useful and leads to a powerful approach to calculate the region *between* the objects of interest based on the concept of visibility. The price to be paid, in this case, is its higher computational cost. In order to derive a more efficient contour-based approach, an alternative model to calculate the *between* region based on convex hulls is introduced, which is less general but still applies to a large class of shapes. For fuzzy objects, we propose an extension of the region-based approach.

We first present a general approach to characterize the *alongness* spatial relation in terms of the region *between* two objects in Section 2. We assume that each object is a connected spatial entity. We propose a mathematical model and measures of *alongness* between crisp objects in Section 3. An efficient contour-based implementation of the convex hull method is described in Section 4. An extension of the general approach to calculate the degree of *alongness* between fuzzy objects is discussed in Section 5. Experimental results using both synthetic and real objects are shown in Section 6. Some properties and possible extensions are provided in Section 7.

2. General approach: *along* as an elongated space *between*

The *between* relation, on which we base our proposal for *along*, is clearly polymorphic and may have different intuitive meanings depending on the objects and their spatial configuration. Similarly the *along* relation may depend on the shape of the objects. To derive the *along* notion from the one of *betweenness* and from the elongatedness of the region between two objects, some assumptions can eventually be made about the objects, such as “at least

one object should be elongated”, or “both objects should be elongated”. Also, the distance between them should be small with respect to the size of the objects. In the example in Fig. 1(a), it can be said that A is along B , or that B is along A . But typically we would not say that A is along B in the example in Fig. 1(b), although the region between them is elongated.

It is quite clear that the region between A and B , denoted by β , should be elongated, as is the case in Fig. 1(a). In our model, we propose a definition that does not necessarily consider the shape of the objects as a whole, that is symmetrical in both arguments, and that involves the region between the objects and their distance. Moreover, as already advocated in [11], defining such relations in a binary way would not be satisfactory, and a degree of satisfaction of the relation is more appropriate. Finally, we also want to be able to deal with situations where the relation is satisfied locally, between parts of the objects only.

Based on these considerations, we propose a mathematical definition of the degree to which an object A is along an object B , based on the region between A and B and a measure of this region. The two main steps of our approach are thus as follows:

1. Calculate the region β between A and B .
2. Measure how elongated is β , thus defining the degree to which A is along B .

One of the interesting features of this approach is that it involves explicitly the *between* region, which is also committed in the usual semantics of the *along* relation. From a mathematical and computational point of view, the approach benefits from powerful existing techniques to calculate the region between A and B . In the present paper we choose to use the definitions proposed in [4]. Once the region between A and B is obtained, the issue of how elongated is β may be treated by shape analysis, leading to different measures which may be chosen depending on the application, as explained below. The paper [4] is used as the basic reference to implement the methods to calculate the *between* region in the present paper.

3. Spatial relation *along* for crisp objects: region-based model

Since no assumption on the shapes of the objects is made, some classical ways to define the *between* region may not be appropriate. Thus, we choose here the visibility approach [4] to model a region-based definition of *betweenness*. In this particular model, concavities of an object that are not visible from the other one are not included in the *between* area.

Conversely, a contour representation may be adopted in order to derive a more computationally efficient method to calculate the *between* region and the *alongness* degree between regions. The visibility approach described above is not completely suitable in this sense because, though the visibility region between two objects may be calculated from their contours, they have to be,

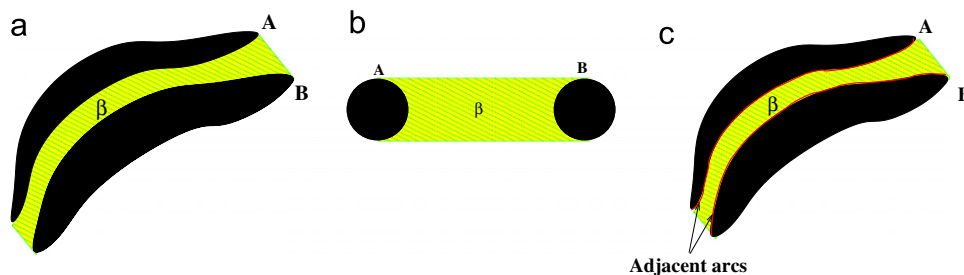


Fig. 1. (a) Example where A is along B , with an elongated region β between A and B . (b) Case where β is elongated but A is not along B . (c) Same example as (a) where adjacent arcs are shown in red. (For interpretation of the references to color in this figure legend, the reader is referred to the web version of this article.)

in principle, defined for each point in the considered 2D image. In order to derive a more efficient method, an alternative approach to calculate the *between* region based on the convex hull [4] and on contour representations is described in Section 4.

In this section, we discuss the region-based model by means of the computation of the region *between* using visibility (Section 3.1) and the elongation (Section 3.2).

3.1. Region between two objects

In [4], methods for computing the region between two objects in order to cope with complex shapes have been proposed, including the visibility approach. More formally, this approach relies on the notion of admissible segments as introduced in [16]. A (straight line) segment $[a, b]$, with a in A and b in B (A and B are supposed to be compact sets or digital objects), is said admissible if it is included in $A^c \cap B^c$ [4]. Note that a and b then necessarily belong to the boundary of A and B , respectively. This has interesting consequences from an algorithmic point of view, since it considerably reduces the size of the set of points to be explored. The traditional Bresenham algorithm has been adopted to calculate the line segments in our experiments. The visible points are those which belong to admissible segments. The region between A and B is then defined as the union of admissible segments.

The second step requires that the extremities (belonging to the boundary of A or B) of the admissible segments are kept in the *between* region. Therefore we slightly modify the definition of [4] as

$$\beta = \bigcup \{[a, b], a \in A, b \in B, [a, b] \text{ admissible}\}. \quad (1)$$

This definition is illustrated in Fig. 2 for two different cases. Note that, in contrast to the objects in Fig. 2(a), in case of Fig. 2(b) there is a concavity in one of the shapes not visible from the other object, which is properly excluded from the *between* region by the visibility approach. This illustrates the agreement between the proposed mathematical definition and the intuitive meaning of the relation.

3.2. Degree of elongatedness

Elongatedness is related to shape measurements and several approaches can be used to define an appropriate measure such as the circularity or the ratio between the minor and the major axes [9]. One of the most popular ones is given by the inverse of compactness, i.e. how elongated is the region with respect to a disk (or more generally a hyper-sphere). This can be measured in the 2D case by the elongatedness measure $c = P^2/S$, where P and S represent the perimeter and the area of the region. We have $c = 4\pi$ for a perfect disk, and the more elongated is the shape, the larger is c . In order to normalize this measure between 0 and 1, we propose a first *alongness* measure defined as

$$\alpha_1 = f_a \left(\frac{P^2(\beta)}{S(\beta)} \right), \quad (2)$$

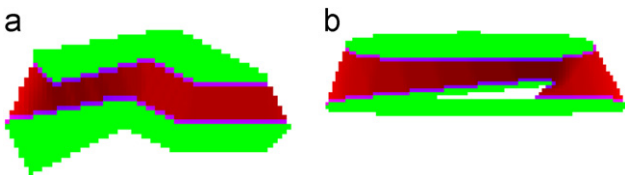


Fig. 2. (a) Region (in red) *between* two objects (in green), calculated by the visibility approach. (b) Another example, showing that the concavity of the object below is properly excluded from the *between* region by the visibility method. (For interpretation of the references to color in this figure legend, the reader is referred to the web version of this article.)

where $S(\beta)$ and $P(\beta)$ denote the area and perimeter of region β , respectively, and f_a is an increasing function, typically a sigmoid, such as $f_a(x) = (1 - \exp(-ax)) / (1 + \exp(-ax))$, which is used in the present paper. This measure α_1 tends towards 1 as β becomes more elongated. Although a is a parameter of the method, f_a is a non-decreasing function that preserves the order, which is the most important property, i.e. a configuration where β is more elongated than in other configurations will always lead to higher values of α_1 . Absolute values can be changed by tuning a to enhance the differences depending on the application.

Let us now introduce the constraints derived from the discussion in Section 2. It is clear that the measure α_1 does not match these constraints. In particular it does not lead to good results in all situations since it considers a global elongatedness, while the elongatedness only in some directions is useful. Let us consider the example in Fig. 1(b). The region between A and B is elongated, but this does not mean that A is along B . On the other hand, the situation in Fig. 1(a) is good since β is elongated in the direction of its adjacency with A and B . In order to model this, instead of using the complete perimeter of β , the total arc length $L(\beta)$ of the contour portions of β adjacent to A or to B is used (see the adjacent arcs indicated in Fig. 1(c)). Here, with the modified definition of β (Eq. (1)), these lines are actually the intersections between A and β and between B and β . The new elongatedness measure is then defined as

$$\alpha_2 = f_a \left(\frac{L^2(\beta)}{S(\beta)} \right). \quad (3)$$

The constraints on distance should now also be considered. Although the measure α_2 produces more adequate results than α_1 , it does not take directly into account the distance between A and B , which is useful in some situations. Also, because α_2 is a global measure over A and B , it fails in identifying if there are some parts of A that are along some parts of B , i.e. it lacks the capability of local analysis. These two potential limitations (depending on the application) are solved by the next two measures, i.e. α_3 (distance) and α_4 (locality), respectively, as shown below.

We propose to incorporate these aspects in the present approach by considering the distance between the two shapes within the *between* area. Let x be an image point, and $d(x, A)$ and $d(x, B)$ the distances from x to A and B respectively (in the digital case, they can be computed in a very efficient way using distance transforms [6,7,17]). Let $D_{AB}(x) = d(x, A) + d(x, B)$. Instead of using the area of β to calculate how elongated it is, we define the volume $V(\beta)$ below the surface $\{(x, D_{AB}(x)), x \in \beta\}$, which is calculated as

$$V(\beta) = \int_{\beta} D_{AB}(x) dx. \quad (4)$$

In the digital case, the integral becomes a finite sum. As an example, see Fig. 6(a), which shows the distance map $D_{AB}(x)$ between the shapes. By taking the region representing $D_{AB}(x)$ as a topographic surface, $V(\beta)$ is calculated as the volume below this topographic surface.

This leads to an *alongness* measure taking into account the distance between A and B :

$$\alpha_3 = f_a \left(\frac{L^2(\beta)}{V(\beta)} \right). \quad (5)$$

The distance $D_{AB}(x)$ may be used in a more refined way in order to deal with situations where just some parts of A can be considered along some parts of B . In such cases, it is expected that such parts are near each other, thus generating a *between* region with lower values of $D_{AB}(x)$. Let $\beta_t = \{x, D_{AB}(x) < t\}$, where t is a distance threshold. Let $L(\beta_t)$, $S(\beta_t)$ and $V(\beta_t)$ be the total adjacent arc length, area and volume for β_t . Two local *alongness* measures,

in the areas which are sufficiently near to each other according to the threshold, are then defined as

$$\alpha_4(t) = f_a \left(\frac{L^2(\beta_t)}{S(\beta_t)} \right) \quad (6)$$

and

$$\alpha_5(t) = f_a \left(\frac{L^2(\beta_t)}{V(\beta_t)} \right). \quad (7)$$

It is important to note that α_3 is similar to α_4 except that points which are farther are disconsidered. Therefore, the measure varies depending on the separation of the two objects.

Note that all measures are dimensionless, except α_3 and α_5 , since V is an integral of distance values over the spatial domain β . For specific applications, it might be preferable to modify these measures, to make them also dimensionless, according to the needs of the application at hand (e.g. by normalizing them by the maximum distance). This question is not further addressed in this paper.

These measures will be tested and compared in Section 6 on synthetic and real objects.

4. Spatial relation along for crisp objects: model based on contours and convex hull

In simple cases (e.g. objects without strong non-visible concavities), a more efficient approach can be derived from a different definition of the between region, based on the convex hull of the union of the two objects. Although this approach presents some limitations with respect to the visibility approach, since it reduces the field of applicability to simple objects, it is interesting because the *between* region can be calculated from the object contours using efficient algorithms, and the computational complexity is reduced from $O(n^2)$ to $O(n)$, where n denotes the number of contour points of the objects.

4.1. Region between two objects

The region *between* two objects may be intuitively related to the convex hull of the union of these objects. Let $CH(X)$ denote the convex hull of X and X^c its complement. The region *between* two objects A_1 and A_2 is defined as [4]

$$\beta_{CH}(A_1, A_2) = CH(A_1 \cup A_2) \cap A_1^c \cap A_2^c. \quad (8)$$

Only the connected components adjacent to A_1 and A_2 should be kept. This constraint and the definition itself are used to derive the contour-based method to calculate the *between* region. The basic idea behind the method is to extract the convex hull of the union of the objects and to identify subsequent points on it which belong to different objects. The contour of the *between* region is composed of an alternate sequence of line segments of the convex hull and the boundary of the two objects. In order to understand the method, refer to Fig. 3, which shows two shapes in (a). The respective contours are shown in Fig. 3(b) and the convex hull of the union of both contours is shown in Fig. 3(c). It is important to note that the convex hull may be represented as a polygonal curve where the vertices touch the original contours. Pairs of subsequent vertices belonging to different objects (as shown by the red dots in Fig. 3(c)) are used to identify the *between* region. These vertices are intersection points between the contour of the convex hull and the contour of the *between* region C_β .

These intersection points lead to the definition of the contour C_β of the *between* region and a straightforward algorithm to extract it. The intersection points divide each contour into two portions called *inner* and *outer* contours, denoted as C_{IN} and C_{OU} , respectively. The inner contours correspond to those contour

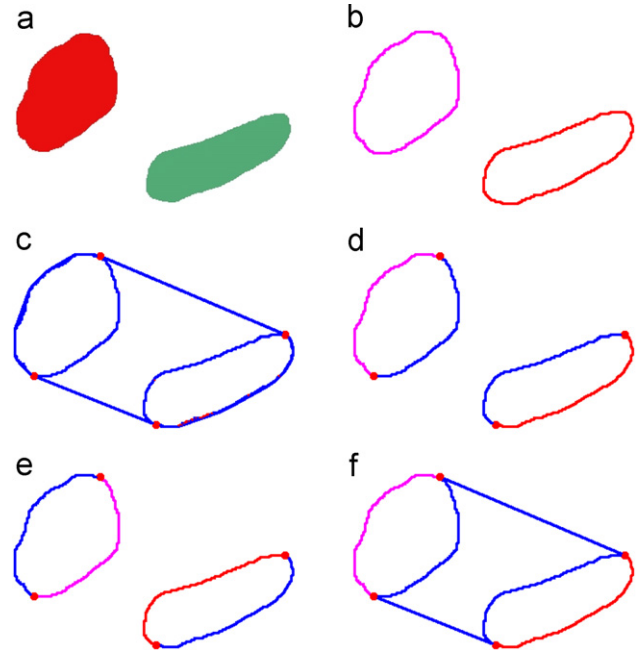


Fig. 3. Contour-based identification of the *between* region: (a) Original image with two objects A_1 (red) and A_2 (green) (the white background represents $A^c \cap B^c$). (b) Respective contours. (c) Convex hull $CH(A_1 \cup A_2)$ with the intersection points between β and CH identified by the red dots. (d) Inner contour C_{IN} marked in blue. (e) Outer contour C_{OU} marked in blue. (f) Contour of the *between* region C_β marked in blue. (For interpretation of the references to color in this figure legend, the reader is referred to the web version of this article.)

portions which belong to C_β (see Fig. 3(d) for an example). Therefore, C_β is composed of an alternate sequence of line segments and inner contour portions. Fig. 4 shows an example of these concepts applied to a real image.

4.2. Degree of elongatedness

The *alongness* measures defined by Eqs. (2) and (3) are suitable to be calculated from the contour of the *between* region C_β . Efficient algorithms to calculate the perimeter and the area from a digital contour are available. The perimeter may be calculated from finite differences between subsequent points. On the other hand, the area A of a polygon C may be calculated in linear time by summing a series of signed triangle areas defined by subsequent pairs of polygonal points. The area A of a polygon C represented by a series of its vertices $v_i = (x_i, y_i)$ may be calculated as

$$A = \frac{1}{2} \sum_{i=0}^{n-1} (x_i y_{i+1} - y_i x_{i+1}), \quad (9)$$

where n is the number of vertices of the polygon and $x_n = x_0$. Eq. (9) may be rearranged in order to decrease the number of multiplications [14]:

$$A = \frac{1}{2} \sum_{i=0}^{n-1} (x_i (y_{i+1} - y_{i-1})). \quad (10)$$

The *alongness* measures may then be calculated as

$$\alpha_{C_1} = P(\beta)^2 / A(\beta), \quad (11)$$

$$\alpha_{C_2} = P(C_{IN})^2 / A(\beta). \quad (12)$$

The notations α_{C_1} and α_{C_2} are used to emphasize the fact that they are calculated using the contour-based representation (as compared to α_1 and α_2 of the region-based approach described in the previous section).

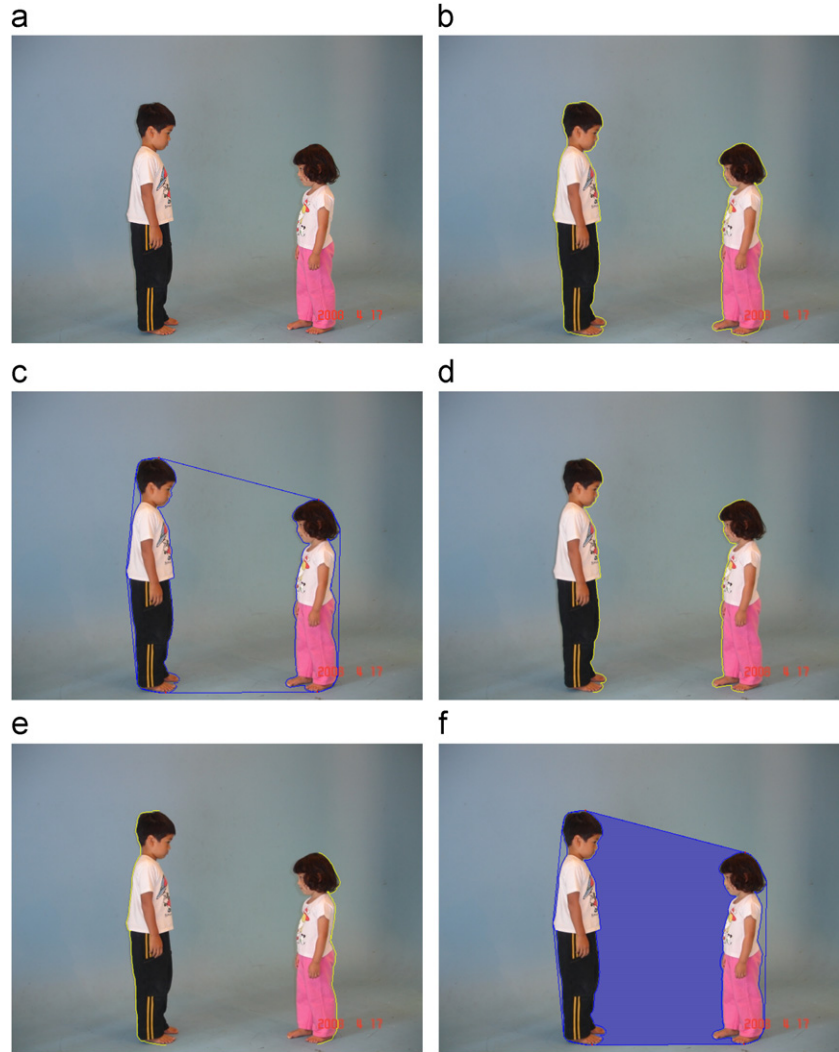


Fig. 4. (a) Original image. (b) Objects contours in yellow. (c) Convex hull CH with the intersection points marked in red. (d) Inner contour C_{IN} marked in yellow. (e) Outer contour C_{OU} marked in yellow. (f) Calculated region β (light blue) between the two children and the corresponding contour C_β (dark blue). (For interpretation of the references to color in this figure legend, the reader is referred to the web version of this article.)

5. Spatial relation along for fuzzy objects

5.1. Region between two objects

Now we consider the case of fuzzy objects, which may be useful to address cases such as spatial imprecision or rough segmentation. We follow the approach in two steps as in the crisp case.

The visibility approach for defining the *between* region can be extended to the fuzzy case by introducing the degree to which a segment is included in $A^C \cap B^C$ (which is now a fuzzy region). Let μ_A and μ_B be the membership functions of the fuzzy objects A and B . The degree of inclusion μ_{incl} of a segment $]a,b[$ in $A^C \cap B^C$ is given by [3,5]

$$\mu_{incl}(]a,b[) = \inf_{y \in]a,b[} \min[1 - \mu_A(y), 1 - \mu_B(y)]. \tag{13}$$

This equation is derived from the degree of inclusion of a fuzzy v in a fuzzy set μ defined as $\inf_y T(1 - v(y), \mu(y))$ where T is a t-conorm, the complementation of μ is taken as $1 - \mu$ and the intersection as the minimum t-norm.

Let us denote the support of the fuzzy objects A and B by $\text{Supp}(A)$ and $\text{Supp}(B)$ respectively. The region between A and B is then defined as the fuzzy set in the spatial domain \mathcal{I} with

membership function β_F :

$$\forall x \in \mathcal{I}, \quad \beta_F(x) = \sup\{\mu_{incl}(]a,b[); a \in \text{Supp}(A), b \in \text{Supp}(B), x \in]a,b[\}, \tag{14}$$

i.e. the maximum inclusion degree of segments $]a,b[$ in $A^C \cap B^C$, among all segments with extremities in A and B and containing x .

5.2. Degree of elongatedness

In order to define *alongness* measures analogous to $\alpha_l, l = 1 \dots 5$, it is necessary to calculate the perimeter, area and volume of β_F . The perimeter $P(\mu)$ and the area $S(\mu)$ of a fuzzy set μ are usually defined as [15]

$$P(\mu) = \int_{\text{Supp}(\mu)} |\nabla \mu(x)| \, dx, \tag{15}$$

where $\nabla \mu(x)$ is the gradient of μ , and

$$S(\mu) = \int_{\text{Supp}(\mu)} \mu(x) \, dx. \tag{16}$$

Similar equations can be derived for the discrete case.

The extension of α_2 requires to define the adjacency region R_{adj} between the objects and β_F . Here we simply consider the union of

the intersection of the supports of A and β_F and the intersection of the supports of B and β_F :

$$R_{adj}(\beta_F, \mu_{A \cup B}) = (\text{Supp}(\beta_F) \cap \text{Supp}(A)) \cup (\text{Supp}(\beta_F) \cap \text{Supp}(B)), \quad (17)$$

where $\mu_{A \cup B}$ represents the union of the fuzzy objects A and B , and extend L as

$$L(\beta_F, \mu_{A \cup B}) = S(R_{adj}(\beta_F, \mu_{A \cup B})). \quad (18)$$

Finally, it is also necessary to calculate the distance of any point x of the *between* region to A and to B . We propose the use of the length of the admissible segments:

$$D_{AB}(x) = \inf\{\|b-a\|, a, b[\text{admissible}, x \in]a, b[\}, \quad \text{for } x \in (\text{Supp}(A) \cup \text{Supp}(B))^c. \quad (19)$$

Then, we define the volume $V(\beta_F)$ below the surface $\{(x, D_{AB}), x \in \beta_F\}$ by weighting each point by its membership to $\beta_F(x)$, as

$$V(\beta_F) = \int_{\text{Supp}(\beta_F)} \beta_F(x) D_{AB}(x) dx. \quad (20)$$

The notation α_{F_i} is used to emphasize the fact that they are calculated using the fuzzy-based representation (as compared to α_i of the region-based approach described previously). The fuzzy *alongness* measures are defined as

$$\alpha_{F_1} = f_a \left(\frac{P^2(\beta_F)}{S(\beta_F)} \right), \quad (21)$$

$$\alpha_{F_2} = f_a \left(\frac{L^2(\beta_F, \mu_{A \cup B})}{S(\beta_F)} \right), \quad (22)$$

$$\alpha_{F_3} = f_a \left(\frac{L^2(\beta_F, \mu_{A \cup B})}{V(\beta_F)} \right), \quad (23)$$

$$\alpha_{F_4}(t) = f_a \left(\frac{L^2(\beta_{F_t}, \mu_{A \cup B})}{S(\beta_{F_t})} \right), \quad (24)$$

$$\alpha_{F_5}(t) = f_a \left(\frac{L^2(\beta_{F_t}, \mu_{A \cup B})}{V(\beta_{F_t})} \right). \quad (25)$$

The interpretation of the above equations is similar to $\alpha_1 - \alpha_5$. The measure α_{F_1} considers the overall elongation while α_{F_2} considers the adjacency region. The distance is taken into account by $\alpha_{F_3} - \alpha_{F_5}$ analogously to $\alpha_3 - \alpha_5$.

In order to keep the fuzzy nature of the model, instead of thresholding the distance function as in the crisp case, we propose to select the closest area based on a decreasing function g of D_{AB} . We thus have $\beta_{F_t}(x) = \beta_F(x)g(D_{AB}(x))$. In our experiments, we have chosen g as

$$g(t) = 1 - f_{a_1}(t), \quad (26)$$

with $a_1 = 0.3$.

6. Experimental results

Extensive results with a large number of pairs of shapes have been successfully produced. Some of these results are presented and discussed in this section.

6.1. Region-based approach applied to crisp objects

Table 1 shows some results obtained on synthetic objects illustrating different situations. The adjacent lines and distance values of the object in Table 1(a) are shown in Fig. 5(a) and (b), respectively. High values of $D_{AB}(x)$ correctly indicate image regions where the shapes are locally far from each other.

Table 1

Alongness values for different shape configurations (synthetic shapes) with parameters $a=0.125$ and $t=10$. A precision of three decimal places was adopted in all results of the paper.

Shapes	(a)	(b)	(c)
α_1	0.907	0.450	0.874
α_2	0.885	0.431	0.340
α_3	0.172	0.011	0.010
$\alpha_4(10)$	0.834	0.653	0.072
$\alpha_5(10)$	0.165	0.127	0.010

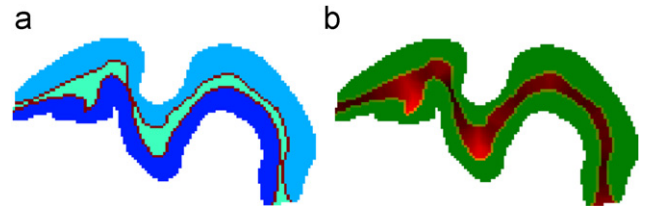


Fig. 5. Results using the visibility approach to calculate β . (a) Synthetic shapes (in blue) and the region β between them (cyan). The adjacent arcs are also indicated in red. (b) The distance map $D_{AB}(x)$ in β is represented as a color map (higher values of $D_{AB}(x)$ are associated to light red colors). (For interpretation of the references to color in this figure legend, the reader is referred to the web version of this article.)

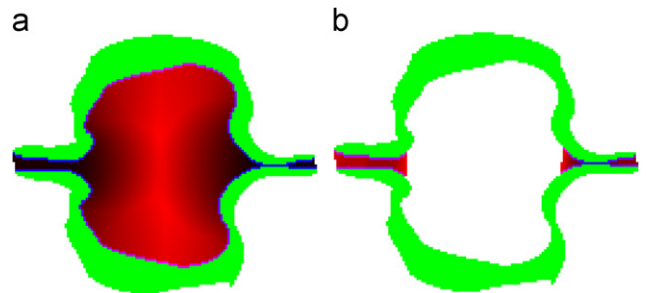


Fig. 6. Results using the visibility approach to calculate β and β_t . (a) The distance map $D_{AB}(x)$ in β is represented as a color map (higher values of $D_{AB}(x)$ are associated to light red colors). (b) The thresholded *between* region $\beta_t = \{x, D_{AB}(x) < t\}$, indicating that only nearby contour portions are taken into account by this approach. (For interpretation of the references to color in this figure legend, the reader is referred to the web version of this article.)

In the example of Table 1(a), the two objects can be considered as along each other, leading to high values of α_1 , α_2 and α_4 . However, some parts of the objects are closer to each other than other parts. When the distance increases, the corresponding parts can hardly be considered as along each other. This is well expressed by the lower values obtained for α_3 and α_5 . These effects are even stronger on the example of Table 1(b) where only small parts of the objects can be considered as being along each other. The *between* regions β and β_t (i.e. thresholded) are shown in Fig. 6.

The third case in Table 1(c) is a typical example where the region between A and B is elongated, but not in the direction of its adjacency with A and B . This is not taken into account by α_1 , while the other measures provide low values as expected: α_2 is much smaller than α_1 and the other three values are almost 0.

Table 2 shows results obtained on real objects, which are some brain structures extracted from magnetic resonance images. Similar values are obtained for all measures in the two first cases where the relation is well satisfied. It is important to emphasize that the modification introduced by the definition of Eq. (1) allows the characterization of adjacent objects (such as in (a) and (b)), since the region between the objects may include the object boundaries. The third example (c) shows the interest of local measures and distance information (in particular the similar values obtained for α_2 and α_4 illustrate the fact that only the parts that are close to each other are actually involved in the computation of the *between* region for this example), while the last one (d) is a case where the relation is not satisfied, which is well reflected by all measures except α_1 , as expected.

6.2. Contour-based approach applied to crisp objects

The contour-based approach has been applied to the same shapes discussed in the previous section. Both synthetic and medical imaging cases have been analyzed. The contours have

Table 2
Alongness values for different shape configurations (brain structures from medical imaging) with parameters $a=0.25$ and $t=10$.

Shapes	(a)	(b)	(c)	(d)
α_1	0.746	0.677	0.487	0.708
α_2	0.746	0.677	0.438	0.289
α_3	0.717	0.611	0.133	0.015
$\alpha_4(10)$	0.746	0.677	0.438	0.001
$\alpha_5(10)$	0.717	0.611	0.133	0.000

been extracted from the segmented images and analyzed by the methods described in Section 4. The results obtained for the contour-based approach (Tables 3 and 4) agree with the region-based approach, for these types of objects. Also refer to the discussion above.




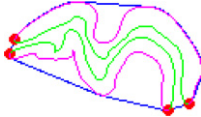
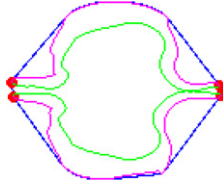
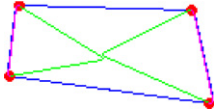



Table 3 shows the analyzed shapes in row (1), the extracted contours and convex hulls in row (2) and the resulting region between the objects in row (3). The results in Table 3 are similar to those in Table 1. In both cases, the shapes that most satisfy the *along* relation are presented in Table 3(a). A case where the *between* region is not elongated is shown in Table 3(b), and this is reflected by the lower values of $\alpha_1, \alpha_2, \alpha_{C_1}$ and α_{C_2} . In Table 3(c), the region *between* is elongated but not in compliance with the *along* definition, which explains the high α_{C_1} value. In this case, α_2 and α_{C_2} are low, thus showing the suitability of this measure.

A similar analysis applies to the cases of real objects in medical imaging shown in Table 4, with similar results as the ones obtained with the region-based approach in Table 2. The object contours are shown in violet, the *between* contour in green and the convex hull in black. α_{C_1} shows expected decreasing values for the cases (a)–(c). However, it fails when applied to the case (d), where a counter-intuitive high satisfaction degree is obtained.

Table 4
Alongness values for different shape configurations (brain structures from medical imaging) for $a=0.0375$. Outer and inner contours and the intersection points are indicated.

Objects	(a)	(b)	(c)	(d)
α_{C_1}	0.798	0.540	0.371	0.718
α_{C_2}	0.628	0.315	0.225	0.282

Table 3
Alongness values for different shape configurations (synthetic fuzzy shapes) with parameter $a=0.05$. (1) Original image. (2) Outer and inner contours, and the corresponding adjacent points with the convex hull identified. (3) Region *between*.

Objects	(a)	(b)	(c)
(1)			
(2)			
(3)			
α_{C_1}	0.965	0.563	0.928
α_{C_2}	0.939	0.516	0.385

This is due to the limitations of α_1 mentioned above, and that led us to propose other measures. In particular in this example, both structures are quite elongated, without being along each other. The second measure avoids this problem by taking into account only the part of β adjacent to the two structures. This leads to a much lower satisfaction degree, as expected.

Table 5 shows the running times of the following procedures: (T_1) calculation of the *between* region using visibility; (T_2) $\alpha_1-\alpha_5$ computation; (T'_1) computation of the *between* region by means of convex hull and contour approach; (T'_2) $\alpha_{C_1}-\alpha_{C_2}$ computation; (T'_3) contour computation. (T) and (T') are the overall execution time of the $\alpha_1-\alpha_5$ and $\alpha_{C_1}-\alpha_{C_2}$ computation, respectively. All values are in seconds. The computer's configuration for these experiments is: AMD Athlon(tm) XP 1500+, 1 G memory. The size of the test

images are (256×256) and the length of the contours is given in Table 5 ($|C_1|$ and $|C_2|$).

The visibility approach was implemented in C, while the convex hull approach using contours was developed in Java. Although it is difficult to perform a precise benchmark using such different implementations, these results are presented to provide some general idea of the differences between the approaches (in terms of running times). The major time consuming step in the computation of $\alpha_1-\alpha_5$ is the computation of the region *between* the objects. In the case of $\alpha_{C_1}-\alpha_{C_2}$, the computational bottleneck is the extraction of the β contour. These experiments indicate that the proposed measures can be efficiently implemented and used in real situations where computational performance is an issue.

6.3. Fuzzy objects

The experiments concerning the fuzzy approach are based on the construction of synthetic fuzzy objects by a Gaussian smoothing of the crisp ones, only for the sake of illustration. In real applications, fuzzy objects may be obtained from a fuzzy segmentation of the image, from imprecision at their boundaries or from partial volume effect modeling, for instance. Fig. 7 illustrates an example of fuzzy objects along with the *between* region and the fuzzy regions β_F and $\beta_{F'}$. The distance map and the selected area are depicted in Fig. 8.

Some results obtained on fuzzy synthetic shapes are given in Table 6, while some results on fuzzy real objects are given in Table 7. In these tables, α_{F_i} denotes the fuzzy equivalent of α_i . The results are again in accordance with what could be intuitively expected, thus showing the consistency of the proposed extension to fuzzy sets.

Since the computation of L , S and V in the fuzzy case is based on the support of the fuzzy objects, which is larger than the corresponding crisp objects, we have to choose a different value for the parameter a , in order to achieve a better discrimination between the different situations. However, a has the same values for all objects in each table, for the sake of comparison. Note that

Table 5
Running time for contour and visibility approaches, given in seconds (see text for notations).

Objects	(a)	(b)	(c)	(d)
Size of contours				
$ C_1 $	205	123	207	219
$ C_2 $	101	121	219	121
Computation time (in seconds)				
T_1	4477	4596	4591	4591
T_2	0	0	0	0
T'_1	0.100	0.114	0.014	0.014
T'_2	0.569	0.270	0.301	0.260
T'_3	0.015	0.008	0.007	0.023
T	4477	4596	4591	4591
T'	0.684	0.392	0.322	0.297

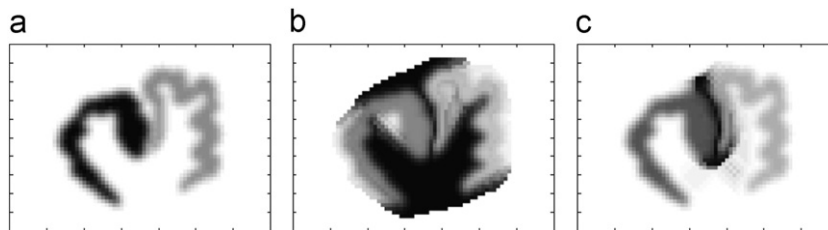


Fig. 7. Results using the fuzzy visibility approach to calculate β_F and $\beta_{F'}$. (a) Original shapes. (b) Shapes and the region β_F between them. (c) Shapes and the thresholded *between* region $\beta_{F'}(x) = \{x, D_{AB}(x) < t\}$.

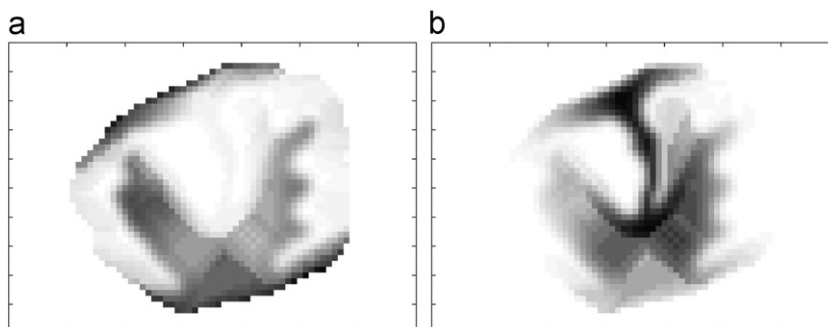


Fig. 8. (a) The distance map $D_{AB}(x)$ in β_F of the objects in Fig. 7(a). (b) The decreasing function g of $D_{AB}(x)$.

Table 6

Alongness values for different shape configurations (fuzzy synthetic shapes) with parameters $\alpha=0.50$ and $\alpha_1=0.30$.

Shapes	(a)	(b)	(c)
α_{F_1}	0.990	0.815	0.982
α_{F_2}	0.999	0.948	0.881
α_{F_3}	0.879	0.531	0.515
α_{F_4}	0.975	0.755	0.572
α_{F_5}	0.686	0.552	0.508

Table 7

Alongness values for different shape configurations (fuzzy brain structures from medical imaging) with parameters $\alpha=0.25$ and $\alpha_1=0.30$.

Shapes	(a)	(b)	(c)	(d)
α_{F_1}	0.996	0.997	0.980	0.997
α_{F_2}	0.984	0.965	0.972	0.971
α_{F_3}	0.888	0.840	0.675	0.536
α_{F_4}	0.812	0.764	0.781	0.544
α_{F_5}	0.675	0.643	0.579	0.503

in Table 6 as well as in Table 7 the results obtained on fuzzy synthetic and real objects are qualitatively the same as the results obtained on crisp objects: in particular, α_{F_3} and α_{F_5} well reflect the distance constraint on the *alongness* degree.

7. Conclusion

We proposed in this paper an original method to model the relation *along* and to compute the degree to which this relation is satisfied between two objects of any shape. Several measures are proposed, taking into account different types of information: region between the objects, adjacency between the objects and this region, distance, parts of objects. The definitions are symmetrical by construction. They inherit some properties of the visibility method for computing the *between* area such as invariance under translation and rotation. Measures α_1 , α_2 and α_4 are also invariant under isotropic scaling. Finally, the proposed measures fit well the intuitive meaning of the relation in a large class of situations, and provide a ranking between different situations which is consistent with the common sense. One of the advantages of the proposed approach is the decomposition of the solution in two parts, i.e. to find the region between the objects and to calculate its elongatedness.

The inverse of compactness (sometimes called circularity) has been adopted to measure how elongated is the region between the shapes. This is by no means the unique way of characterizing elongatedness. In fact, if the region between the shapes becomes very complex (e.g. Fig. 9), the area starts to increase fast with respect to the perimeter (i.e. space-filling property), and circularity-based measures may produce poor results. In such cases, alternative elongatedness measures may be adopted to replace circularity in our proposed approach (e.g. shape measures that characterize thinness of a shape).

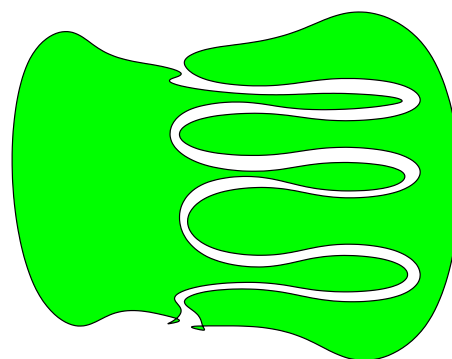


Fig. 9. The two complex shapes (in green) lead to a space-filling *between* region. This may affect the circularity-based elongatedness measure, thus requiring alternative approaches to evaluate how elongated is the *between* region. (For interpretation of the references to color in this figure legend, the reader is referred to the web version of this article.)

Alternative approaches to the computation of length of the adjacent regions and distances can be tested. We can restrict, for example, the adjacent region to the watershed line of this intersection, and compute its length in a classical way. On the other hand, instead of using Eq. (19), we can calculate $D_{\mu_{A \cup B}}$ with the distances to the α -cuts. The distance $d(x, \mu)$ from a point x to a fuzzy set with membership function μ can indeed be defined by integrating over α the distance from x to each α -cut. Another option is to calculate $d(x, \mu)$ as the distance of x to the support of μ , i.e. $d(x, \mu) = d(x, \text{Supp}(\mu))$. These definitions are useful for implementation purposes since for each α -cut, a fast distance transform can be used.

Extensions to 3D are straightforward: the computation of the *between* relation does not make any assumption on the dimension of space; the measures of elongatedness can be simply performed by replacing lengths by surfaces and surfaces by volumes.

In the present paper, we are not addressing the case of disconnected objects, which is an important situation. For instance, refer to Fig. 1 and suppose the situation of a series of A_i s and B_i s in a row, which would mean that $\{A_i\}$ is along $\{B_i\}$. This is an important topic that should be addressed in future works, possibly taking into account grouping and perceptual analysis (i.e. where a series of connected components are perceived as a single object).

Future work also aims at introducing this relation as a new feature in structural pattern recognition or content-based image retrieval schemes.

Acknowledgements

The authors are grateful to FAPESP, CNPq, CAPES, FINEP and COFECUB for financial support.

References

- [1] I. Biederman, Recognition-by-components: a theory of human image understanding, *Psychological Review* 94 (2) (1987) 115–147.
- [2] I. Bloch, On fuzzy spatial distances, in: P. Hawkes (Ed.), *Advances in Imaging and Electron Physics*, vol. 128, Elsevier, Amsterdam, 2003, pp. 51–122.
- [3] I. Bloch, Fuzzy spatial relationships for image processing and interpretation: a review, *Image and Vision Computing* 23 (2) (2005) 89–110.
- [4] I. Bloch, O. Colliot, R.M. Cesar Jr., On the ternary spatial relation “between”, *IEEE Transactions on Systems, Man and Cybernetics Part B—Cybernetics* 36 (2) (2006) 312–327.
- [5] I. Bloch, H. Maître, Fuzzy mathematical morphologies: a comparative study, *Pattern Recognition* 28 (9) (1995) 1341–1387.
- [6] G. Borgefors, Distance transformations in digital images, *Computer Vision, Graphics, and Image Processing* 34 (1986) 344–371.

- [7] H. Breu, J. Gil, D. Kirkpatrick, M. Werman, Linear time Euclidean distance transform algorithms, *IEEE Transactions on Pattern Analysis and Machine Intelligence* 17 (5) (1995) 529–533.
- [8] E. Clementini, P.D. Felice, D. Hernandez, Qualitative representation of positional information, *Artificial Intelligence* 95 (1997) 317–356.
- [9] L. Costa, R. Cesar Jr., *Shape Analysis and Classification: Theory and Practice*, 2nd ed., CRC Press, 2009.
- [10] D. Crevier, A probabilistic method for extracting chains of collinear segments, *Computer Vision and Image Understanding* 76 (1) (1999) 36–53.
- [11] J. Freeman, The modelling of spatial relations, *Computer Graphics and Image Processing* 4 (1975) 156–171.
- [12] J.E. Hummel, I. Biederman, Dynamic binding in a neural network for shape recognition, *Psychological Review* 99 (3) (1992) 480–517.
- [13] B.J. Kuipers, T.S. Levitt, Navigation and mapping in large-scale space, *AI Magazine* 9 (2) (1988) 25–43.
- [14] J. O'Rourke, *Computational Geometry in C*, Cambridge University Press, New York, NY, USA, 1994.
- [15] A. Rosenfeld, The fuzzy geometry of image subsets, *Pattern Recognition Letters* 2 (1984) 311–317.
- [16] A. Rosenfeld, R. Klette, Degree of adjacency or surroundedness, *Pattern Recognition* 18 (2) (1985) 169–177.
- [17] A. Rosenfeld, J.L. Pfaltz, Sequential operations in digital picture processing, *Journal of ACM* 13 (4) (1966) 471–494.
- [18] A.R. Shariff, M. Egenhofer, D. Mark, Natural-language spatial relations between linear and areal objects: the topology and metric of English-language terms, *International Journal of Geographical Information Science* 12 (3) (1998) 215–246.
- [19] A.M. Treisman, Strategies and models of selective attention, *Psychological Review* 76 (3) (1969) 282–299.
- [20] M.E. Wheeler, A.M. Treisman, Binding in short-term visual memory, *Journal of Experimental Psychology* 131 (1) (2002) 48–64.

Celina M. Takemura is a researcher at Embrapa Satellite Monitoring's Technology Transfer Department. She works mainly with Innovation Management, and her research interests include shape analysis, structural pattern recognition and spatial reasoning.

Roberto M. Cesar Jr. is Professor at DCC – IME – USP, Brazil. His main research topics include shape analysis, computer vision, pattern recognition and computational biology.

Isabelle Bloch is Professor at Télécom ParisTech. Her research interests include 3D image and object processing, 3D and fuzzy mathematical morphology, decision theory, information fusion, fuzzy set theory, belief function theory, structural pattern recognition, spatial reasoning, and medical imaging.